Calcicludine Binding to the Outer Pore of L-type Calcium Channels Is Allosterically Coupled to Dihydropyridine Binding†

Xianming Wang, Lei Du, and Blaise Z. Peterson*

Department of Cellular and Molecular Physiology, The Penn State Milton S. Hershey College of Medicine, Hershey, Pennsylvania 17033

Received January 26, 2007; Revised Manuscript Received April 12, 2007

ABSTRACT: How dihydropyridines modulate L-type voltage-gated Ca^{2+} channels is not known. Dihydropyridines bind cooperatively with Ca^{2+} binding to the selectivity filter, suggesting that they alter channel activity by promoting structural rearrangements in the pore. We used radioligand binding and patch-clamp electrophysiology to demonstrate that calcicludine, a toxin from the venom of the green mamba snake, binds in the outer vestibule of the pore and, like Ca^{2+}, is a positive modulator of dihydropyridine binding. Data were fit using an allosteric scheme where dissociation constants for dihydropyridine and calcicludine binding, K_{DHP} and K_{CaC}, are linked via the coupling factor, α. Nine acidic amino acids located within the S5-Pore-helix segment of repeat III were sequentially changed to alanine in groups of three, resulting in the mutant channels, Mut-A, Mut-B, and Mut-C. Mut-A, whose substitutions are proximal to IIIS5, exhibits a 4.5-fold reduction in dihydropyridine binding and is insensitive to calcicludine binding. Block of Mut-A currents by calcicludine is indistinguishable from wild-type, indicating that K_{CaC} is unchanged and that the coupling between dihydropyridine and calcicludine binding (i.e., α) is disrupted. Mut-B and Mut-C possess K_{DHP} values that resemble that of the wild type. Mut-C, the most C-terminal of the mutant channels, is insensitive to calcicludine binding and block. K_{CaC} values for the Mut-C single mutants, E1122A, D1127A, and D1129A, increase from 0.3 (wild type) to 1.14, 2.00, and 20.5 μM, respectively. Together, these findings suggest that dihydropyridine antagonist and calcicludine binding to L-type Ca^{2+} channels promote similar structural changes in the pore that stabilize the channel in a nonconducting, blocked state.

The flow of Ca^{2+} ions through voltage-gated Ca^{2+} channels drives a variety of cellular processes including excitation−contraction coupling, neurotransmitter release, and gene expression. Voltage-activated Ca^{2+} channels are heteromultimeric complexes consisting of α_1, β, α_2/δ, and sometimes γ subunits. The pore-forming α_1 subunit contains all of the structural determinants required for voltage-dependent gating, drug binding, and ion permeation. The membrane topology of the α_1 subunit consists of four homologous repeats (I, II, III, and IV), each consisting of six transmembrane segments (S1−S6). Each of the four S5/S6 connecting segments contains a highly conserved negatively charged glutamate residue that together form a binding site for Ca^{2+} ions called the selectivity filter. The selectivity filter is the narrowest region in the pore and is the site that enables the channel to conduct Ca^{2+} ions under physiological conditions where Na^+ is in excess (*1*).

L-type $Ca_V1.2$ Ca^{2+} channels are targeted by numerous small organic molecules including the dihydropyridines (DHPs[1]). DHPs are allosteric modulators of Ca^{2+} channels and can behave either as agonists or antagonists. Despite much research spanning over two decades, the molecular details that underlie DHP action are still a mystery. Localizing the DHP receptor site was an important step toward developing an understanding of how DHPs interact with and modulate L-type Ca^{2+} channels. DHPs are small lipophilic compounds that have a strong tendency to associate with lipid bilayers (*2*). Kass and colleagues found that the DHP receptor site lies within the lipid bilayer approximately 11−14 Å from the extracellular surface of the membrane (*3*). These conclusions are consistent with mutagenic studies where individual amino acid residues located on transmembrane segments IIIS5, IIIS6, and IVS6 were found to be critical for DHP binding and activity (*4*−*8*).

Important clues regarding the molecular basis for DHP action came from the finding that DHP binding to a site that lies outside the permeation pathway is cooperative with Ca^{2+} binding to the selectivity filter, suggesting that the binding of DHPs and Ca^{2+} promotes reciprocal structural rearrangements in the outer pore that alter the functional behavior of the channel (*9*, *10*). Two recent studies using independent approaches, radioligand binding and whole-cell patch-clamp electrophysiology, suggest that DHPs block monovalent and divalent currents by stabilizing a nonconducting blocked state that is structurally and functionally analogous to a channel with a single Ca^{2+} ion in its selectivity filter (*11*, *12*). It is expected that the elusive molecular mechanisms that underlie DHP activity can be revealed by gaining a deeper understanding of the structural features of the conducting and nonconducting blocked states of the Ca^{2+} channel.

† This work was supported by research grants from the American Heart Association (0230298N) and the National Institutes of Health (RO1 HL074143) to B.Z.P.

* To whom correspondence should be addressed. Department of Cellular and Molecular Physiology (H-166), The Penn State Milton S. Hershey College of Medicine, 500 University Drive, Hershey, PA 17033. Phone: (717) 531-8569. Fax: (717) 531-7667. E-mail: bpeterson@psu.edu.

[1] Abbreviations: DHP, dihydropyridine; EEEE locus, selectivity filter; PN200-110, 4-(4-benzofurazanyl)-1,4-dihydro-2,6-dimethyl-3,5-pyridinedicarboxylic acid methyl 1-methylester.

10.1021/bi7001696 CCC: $37.00
Published on Web 05/31/2007

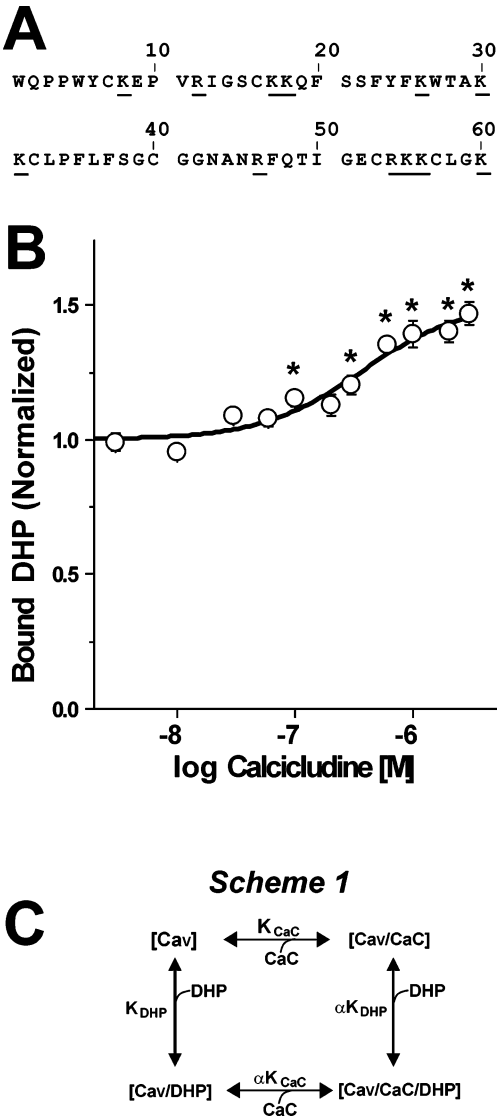

FIGURE 1: Calcicludine is a positive allosteric modulator of DHP binding. (A) Primary sequence of calcicludine. Calcicludine is a 60 amino acid peptide containing three disulfide bonds, 12 positively charged lysine or arginine residues (underlined) and two negatively charged glutamate residues. (B) Membranes from cells expressing wild-type $Ca_V1.2$ Ca^{2+} channels were incubated with ~350 pM [^{3}H]PN200-110 and increasing concentrations of calcicludine. Each experiment was fit using Scheme 1 (see eq 4, Materials and Methods) and normalized such that the occupancy in zero calcicludine is equal to 1.0. Note that [^{3}H]PN200-110 binding increases as calcicludine is raised from 3 nM to 3 μM. Binding data are the means ± SEM, and calcicludine concentrations where DHP binding differs significantly from that with no toxin (determined by ANOVA) are indicated with asterisks (*; $P < 0.05$; $n = 6$). Error bars smaller than symbols do not appear in the Figure. (C) Allosteric binding model for DHP and calcicludine binding. See Materials and Methods and text for details.

Toxins from a wide range of organisms bind to voltage-gated Ca^{2+} channels (*1*, *13*). Calcicludine, a toxin from the venom of the green mamba snake (*Dendroaspis angusticeps*), is a 60 amino acid peptide that consists of 3 disulfide bonds, 12 positively charged arginine or lysine residues, and only 2 negatively charged glutamate residues (Figure 1A). Because of its folding pattern, calcicludine is classified as a bovine pancreatic trypsin inhibitor (BPTI)/Kunitz-like toxin (*14*−*17*) and is structurally homologous to the K^+ channel selective dendrotoxins (*18*).

Schweitz et al. reported that N- and P/Q-type currents are effectively blocked by calcicludine (*16*). In contrast, Stotz et al. found that currents through $Ca_V2.1$, $Ca_V2.2$, and $Ca_V2.3$ Ca^{2+} channels are only modestly inhibited (<10%) by 100 nM calcicludine (*19*). Chimeric Ca^{2+} channels were constructed to identify which domains of $Ca_V1.2$ contain calcicludine binding determinants (*19*). The level of block was reduced through chimeric channels where domains I, II, and III of $Ca_V1.2$ were individually replaced with the corresponding regions of $Ca_V2.3$. These findings led the authors to conclude that calcicludine interacts with all three domains of $Ca_V1.2$. The greatest effects were observed using the domain III chimera (*19*).

We hypothesized that if calcicludine does indeed interact with the outer pore of $Ca_V1.2$, it may act as a modulator of DHP binding, as was observed for the binding of a single Ca^{2+} ion to the selectivity filter (*9*, *10*, *12*). Thus, calcicludine could be used as a molecular probe to study the structural rearrangements associated with DHP binding and could aid in the development of a deeper understanding of the molecular events that couple DHP binding to changes in channel block. Here, we (1) demonstrate that calcicludine and DHP antagonists bind cooperatively to $Ca_V1.2$ channels; (2) identify three acidic amino acid residues located in the outer vestibule of domain III that are critical calcicludine binding determinants; and (3) identify a cluster of acidic residues positioned at the carboxyl terminus of IIIS5 that are important for DHP (but not calcicludine) binding and the coupling between DHP and calcicludine binding. These findings are described using an allosteric binding model. We propose that DHP and calcicludine binding to their respective binding sites blocks currents through L-type Ca^{2+} channels by promoting similar structural rearrangements in the outer pore that stabilize the channel in a nonconducting state.

MATERIALS AND METHODS

Construction and Expression of Mutant Ca^{2+} Channels. cDNAs encoding wild-type (*20*) and mutant $Ca_V1.2$ Ca^{2+} channels were co-transfected with β_{2a} (*21*) and $\alpha_2\delta$ (*22*) into HEK293 cells by calcium phosphate precipitation as described previously (*23*). All cDNAs were expressed in the expression plasmid, pCDNA3 (Invitogen, Carlsbad, CA). Mutant α_{1C} subunits were constructed by site-directed mutagenesis using polymerase chain reaction. Briefly, a NheI site was introduced by silent mutagenesis into the pore of domain III at amino acid positions 1131 and 1132. Mutagenic reverse primers and a forward primer lying upstream of an existing EcoRI site in domain II were used in single polymerase chain reactions. The resulting PCR products were amplified using the TOPO ZeroBlunt Cloning System (Invitrogen, Carlsbad, CA). Mutant inserts were excised by EcoRI/NheI digestion and ligated into EcoRI/NheI-digested $Ca_V1.2$ vector. The integrity of the resulting mutant cDNAs was confirmed DNA sequence analysis. The general gating properties of the mutant channels used in these studies are indistinguishable from those of the wild type.

Membrane Preparation and Radioligand Binding. Membranes were harvested 2 to 3 days following transfection. Cells were washed twice, transferred to a glass−tephlon homogenizer, and homogenized on ice in binding buffer (50 mM Tris, 100 μM phenylmethylsulfonyl fluoride, 100 μM

benzamidine, 1.0 μM pepstatin A, 1.0 μg/μL leupeptin, and 2.0 μg/mL aprotinin at pH 8.0). The homogenate was centrifuged at 1700*g* for 10 min at 4 °C, and the resulting pellet was re-homogenized and centrifuged. The final pellet was discarded, and the supernatants were combined and centrifuged at 100,000*g* at 4 °C for 30 min. The resulting membrane pellet was washed and homogenized in binding buffer. Membrane aliquots were stored at −70 °C and remained stable for several months as determined by radioligand binding but were typically used within one week of harvesting.

Saturation binding assays were performed in binding buffer, 1 mM $CaCl_2$, 20−100 μg of membrane protein, and 0.1−10 nM (+)-[^{3}H]PN200-110 (PerkenElmer Life and Analytical Sciences, Boston, MA). Reactions were incubated for 2 h at 22−24 °C, and each data point was determined by three replicates. No specific binding was detected using membranes from untransfected cells. Assays designed to evaluate the cooperativity between DHP and calcicludine binding were performed in binding buffer, 1 mM $CaCl_2$, 20−100 mg of membrane protein, and the indicated concentrations of calcicludine (Alomone Labs, Tel Aviv, Isreal), and each data point was determined by four replicates. After 30 min at 22−24 °C, (+)-[^{3}H]PN200-110 was added at a concentration equal to K_{DHP}. This concentration of (+)-[^{3}H]-PN200-110 produces a fractional occupancy of 0.5 in the absence of calcicludine. Nonspecific binding was determined in all experiments by the addition of 1 μM (±)PN200-110, thus reducing the k_{on} for the radiolabeled ligand to an insignificant level. Bound radioligand was recovered by vacuum filtration through GF/C glass fiber filters.

DHP binding as a function of calcicludine concentration was fit using Scheme 1 (Figure 1) with the aid of the analysis and graphics programs EXCEL (Microsoft, Redmond, WA) and ORIGIN (OriginLab Corp., Northampton, MA). K_{DHP} and K_{CaC} can be determined from Scheme 1 using the following relationships:

$$K_{DHP} = \frac{DHP[Ca_V]}{[Ca_V{\cdot}DHP]} = \frac{DHP[Ca_V{\cdot}CaC]}{\alpha[Ca_V{\cdot}DHP{\cdot}CaC]}$$

$$K_{CaC} = \frac{CaC[Ca_V]}{[Ca_V{\cdot}CaC]} = \frac{CaC[Ca_V{\cdot}DHP]}{\alpha[Ca_V{\cdot}DHP{\cdot}CaC]}$$

where K_{DHP}, K_{CaC}, and α correspond to the dissociation constants for [^{3}H]PN200-110 (DHP) and calcicludine (CaC) and a unitless coupling factor (α), respectively, that is a measure of the strength of the cooperativity between the DHP and calcicludine binding sites. [Ca_V], [$Ca_V{\cdot}DHP$], [$Ca_V{\cdot}CaC$], and [$Ca_V{\cdot}DHP{\cdot}CaC$] correspond to binding states with no ligand, only DHP, only calcicludine, and both DHP and calcicludine, respectively, bound to the channel. The population of $Ca_V1.2$ channels is distributed between each of the four binding states depicted in Scheme 1, and the fractional occupancies of all four states add to one as follows.

$$1 = [Ca_V] + [Ca_V{\cdot}CaC] + [Ca_V{\cdot}DHP] + [Ca_V{\cdot}DHP{\cdot}CaC] \quad (1)$$

The above relationships can be used to describe each binding state depicted in eq 1.

$$[Ca_V] = \frac{K_{DHP}[Ca_V{\cdot}DHP]}{DHP} = \frac{K_{CaC}[Ca_V{\cdot}CaC]}{CaC}$$

$$[Ca_V{\cdot}CaC] = \frac{\alpha K_{DHP}[Ca_V{\cdot}DHP{\cdot}CaC]}{DHP} = \frac{K_{DHP}CaC[Ca_V]}{K_{CaC}}$$

$$[Ca_V{\cdot}DHP] = \frac{DHP[Ca_V]}{K_{DHP}} = \frac{K_{CaC}[Ca_V{\cdot}DHP{\cdot}CaC]}{CaC}$$

$$[Ca_V{\cdot}DHP{\cdot}CaC] = \frac{DHP[Ca_V{\cdot}CaC]}{\alpha K_{DHP}} = \frac{CaC[Ca_V{\cdot}DHP]}{\alpha K_{CaC}}$$

Of these four binding states, only [$Ca_V{\cdot}DHP$] and [$Ca_V{\cdot}DHP{\cdot}CaC$] are represented in radioligand binding experiments (i.e., total bound = [$Ca_V{\cdot}DHP$] + [$Ca_V{\cdot}DHP{\cdot}CaC$]). The occupancy of state [$Ca_V{\cdot}DHP$] is solved by the following equation.

$$1 = \frac{K_{DHP}[Ca_V{\cdot}DHP]}{DHP} + \frac{K_{DHP}CaC[Ca_V{\cdot}DHP]}{K_{CaC}DHP} + [Ca_V{\cdot}DHP] + \frac{CaC[Ca_V{\cdot}DHP]}{\alpha K_{CaC}}$$

Divide by [$Ca_V{\cdot}DHP$] to obtain the following equation.

$$\frac{1}{[Ca_V{\cdot}DHP]} = \frac{K_{DHP}}{DHP} + \frac{K_{DHP}CaC}{K_{CaC}DHP} + 1 + \frac{CaC}{\alpha K_{CaC}} \quad (2)$$

The occupancy of state [$Ca_V{\cdot}DHP{\cdot}CaC$] is solved by the following equation.

$$1 = \frac{\alpha K_{DHP}K_{CaC}[Ca_V{\cdot}DHP{\cdot}CaC]}{DHP{\cdot}CaC} + \frac{\alpha K_{DHP}[Ca_V{\cdot}DHP{\cdot}CaC]}{DHP} + \frac{\alpha K_{CaC}[Ca_V{\cdot}DHP{\cdot}CaC]}{CaC} + [Ca_V{\cdot}DHP{\cdot}CaC]$$

Divide by [$Ca_V{\cdot}DHP{\cdot}CaC$] to obtain the following equation.

$$\frac{1}{[Ca_V{\cdot}DHP{\cdot}CaC]} = \frac{\alpha K_{DHP}K_{CaC}}{DHP{\cdot}CaC} + \frac{\alpha K_{DHP}}{DHP} + \frac{\alpha K_{CaC}}{CaC} + 1 \quad (3)$$

The sum of the inverses of eqs 2 and 3 is a measure of the total bound [^{3}H]PN200-110 at any given concentration of calcicludine and [^{3}H]PN200-110.

$$\text{Occupancy} = \frac{1}{\frac{K_{DHP}}{DHP} + \frac{K_{DHP}CaC}{K_{CaC}DHP} + 1 + \frac{CaC}{\alpha K_{CaC}}} + \frac{1}{\frac{\alpha K_{DHP}K_{CaC}}{DHP{\cdot}CaC} + \frac{\alpha K_{DHP}}{DHP} + \frac{\alpha K_{CaC}}{CaC} + 1} \quad (4)$$

Equation 4 was used to fit the binding data depicted in Figures 1B and 3A and B.

Patch-Clamp Electrophysiology. Whole-cell currents were recorded at room temperature 2 to 3 days after transfection. Pipettes were pulled from borosilicate glass (1B150F-3; World Precision Instruments, Inc., Sarasota, FA) using a

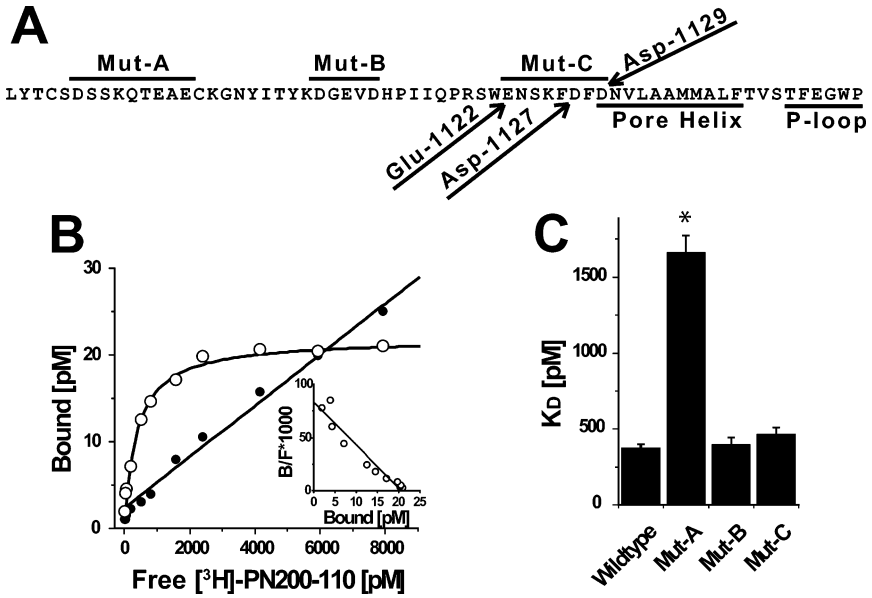

FIGURE 2: Acidic residues proximal to the extracellular portion of IIIS5 are important binding determinants for [^{3}H]PN200−110. (A) Amino acid sequence of $Ca_V1.2$ beginning at the C-terminus of IIIS5 through the pore loop. Peptide segments corresponding to regions spanned by Mut-A, Mut-B, and Mut-C are indicated by lines above the sequence. Glu-1122, Asp-1127, and Asp-1129 are indicated by arrows. The pore helix and P-loop are indicated by lines below the sequence. (B) Saturation binding experiment using membranes derived from cells expressing wild-type $Ca_V1.2$ channels was performed as described in Materials and Methods. The signal-to-noise ratio can be assessed by comparing the relative levels of specific (○) and nonspecific (●) binding. (Inset) Scatchard transformation of data from panel B indicates that the cells express a single population of high affinity receptor sites. (C) Similar analyses were performed on independent membrane preparations derived from cells expressing wild-type ($n = 6$), Mut-A ($n = 3$), Mut-B ($n = 3$), and Mut-C ($n = 3$) channels (see Table 1).

Sutter P-97 Flaming/Brown micropipette puller (Sutter Instruments Company, Novato, CA) and fire polished using a MF200 microforge (World Precision Instruments, Inc., Sarasota, FA). Pipet resistances were typically 2.5−3.0 MΩ. External solutions for whole-cell recordings contained (in mM) NMG-aspartate, 130; HEPES, 10; 4-aminopyridine, 10; glucose, 10; and $BaCl_2$, 10. The internal solutions contained (in mM) NMG-$MeSO_3$, 140; EGTA, 10; $MgCl_2$, 1; MgATP, 4; and HEPES, 10. The osmolarity and pH of internal and external solutions were adjusted to 300 mmol/kg and 7.4, respectively. Data were acquired using a HEKA Epc9/2 amplifier and PULSE/PULSEFIT software (ALA Scientific Instruments, Inc., Westbury, NY). Currents were sampled at 10 kHz and filtered at 2 kHz. Series resistance was typically <6 MΩ and was compensated by ∼70%. Leaks and capacitive transients were subtracted using a P/4 protocol. A homemade rapid-exchange, single-cell perfusion system was used to increase the external solution exchange rates, thus minimizing undesirable effects resulting from current rundown, and to minimize toxin consumption.

The statistical significance of the observed differences between the blocking parameters of wild-type and mutant channels was evaluated using a 2-tailed Students *t* test. All data are means ± SEM and statistical significance was set at $P < 0.05$ (*). Error bars smaller than symbols do not appear in Figures.

RESULTS

Calcicludine is a Positive Allosteric Modulator of DHP Binding. Crude membranes from HEK 293 cells expressing wild-type $Ca_V1.2$ L-type Ca^{2+} channels were incubated with the DHP antagonist, [^{3}H]PN200-110, and concentrations of calcicludine ranging from 3 nM to 3 μM (Figure 1B). Calcicludine increases DHP binding by 51% with an EC_{50} of 372 nM, a value 4.5-fold higher than that reported for rat brain $Ca_V1.2$ Ca^{2+} channels expressed in HEK 293 cells (*19*). That calcicludine increases [^{3}H]PN200-110 binding indicates that the two ligands bind to the Ca^{2+} channel simultaneously and do not compete for the same binding site. The binding data in Figure 1B were fit using the allosteric binding model depicted in Figure 1C (Scheme 1; eq 4) where a single DHP receptor site is shown to transition between two affinity states (i.e., K_{DHP} and αK_{DHP}), and calcicludine binding to its receptor site shifts the equilibrium between these states to the right, thus stabilizing the high affinity state (i.e., αK_{DHP}). DHP and calcicludine binding are linked in Scheme 1 by the coupling factor α, which is a unitless measure of the strength of the coupling between the two sites. Scheme 1 allows one to determine the dissociation constant for DHP binding at any calcicludine concentration and, conversely, the dissociation constant for calcicludine binding at any DHP concentration.

To better understand the positive cooperativity between the DHP and calcicludine binding sites and how each ligand interacts with specific structural determinants to alter the functional behavior of the Ca^{2+} channel, we used site-directed mutagenesis to localize individual amino acid determinants for calcicludine binding. We chose to limit this screen for calcicludine binding determinants to acidic residues in the segment connecting S5 to the selectivity filter in domain III (the IIIS5/P segment) for the following reasons: (1) our previous studies indicate that non-glutamate amino acid residues in the pore of domain III are associated with structural changes that occur upon DHP binding (*12*, *23*); (2) analysis of chimeric $Ca_V1.2/Ca_V2.3$ Ca^{2+} channels suggests that domain III possesses the most important

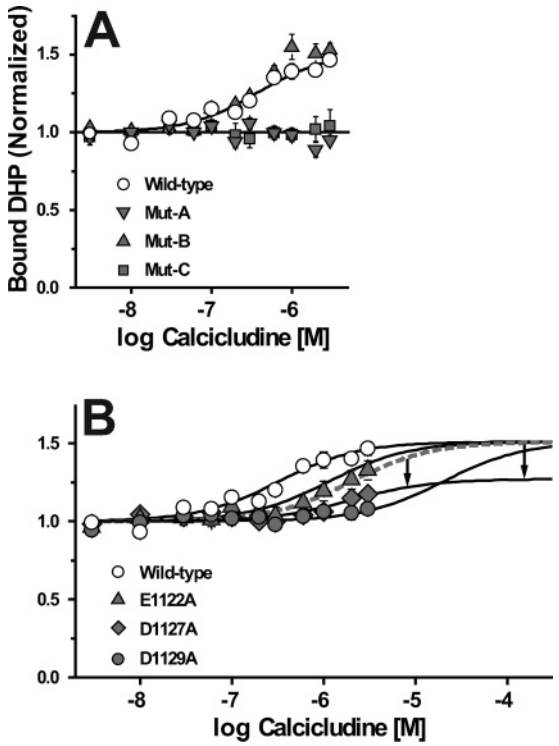

FIGURE 3: Three acidic amino acid residues, Glu-1122, Asp-1127, and Asp-1129, positioned proximal to the pore helix in domain III are important for calcicludine binding to $Ca_V1.2$ channels. Wild-type, Mut-A, Mut-B, and Mut-C (A) and wild-type, E1122A, D1127A, and D1129A (B) Ca^{2+} channels were incubated with [^{3}H]-PN200-110 and the indicated concentrations of calcicludine as described in Materials and Methods. Data were fit using Scheme 1 (see eq 4, Materials and Methods) and normalized such that the occupancy in zero calcicludine is equal to 1.0. The method for fitting binding data from the individual mutants, E1122A, D1127A, and D1129A, is described in the text and footnote to Table 1. DHP binding to Mut-A and Mut-C membranes does not increase in the presence of calcicludine, but block of Mut-A and not Mut-C currents by calcicludine is similar to that of the wild type (Figure 5; see text for details). Data are the means ± SEM, and significant differences between binding parameters of the wild-type and mutant channels were evaluated using a 2-tailed Students *t*-test $P < 0.05$ (*). Error bars smaller than symbols do not appear in the Figure. See Table 1 for the data summary and indications of statistical significance. (A) Wild-type ($n = 6$), Mut-A ($n = 3$), Mut-B ($n = 3$), and Mut-C ($n = 3$); (B) wild-type ($n = 6$), E1122A ($n = 3$), D1127A ($n = 3$), and D1129A ($n = 3$).

Table 1: Binding Parameters for Wild-Type and Mutant Ca^{2+} Channels[a]

	K_{DHP} (pM)	K_{CaC} (αM)	a
wild-type	367 ± 19	0.322 ± 0.055	0.48 ± 0.05
Mut A	1660 ± 120[b]	0.344 ± 0.065	~1[b]
Mut B	391 ± 52	0.216 ± 0.024	0.45 ± 0.05
Mut C	460 ± 50	n.d.	n.d.
E1122A	294 ± 42	1.14 ± 0.20[b]	n.d.
D1127A	511 ± 53	1.61 ± 0.94[b]	0.75 ± 0.07[b]
D1129A	289 ± 80	21.0 ± 6.0[b]	n.d.

[a] K_{DHP} values were determined by [^{3}H]-PN200-110 binding in the absence of calcicludine, as described in Figure 2. K_{CaC} values were determined using whole-cell patch-clamp electrophysiology, as described in Figures 4 and 5. Values for the cooperativity factor alpha (α) for wild-type, Mut A, and Mut B were determined by fitting the data depicted in Figure 3. Mut C proved to be insensitive to calcicludine; therefore, K_{CaC} and α for this mutant were not determined (n.d.). Binding data from E1122A and D1129A were fit using the mutants' respective K_{DHP} and K_{CaC} values and a value for α equal to that of wild-type (i.e., 0.48). In contrast to E1122A and D1129A, it was necessary to adjust α to 0.75 to achieve a reasonable fit for D1127A. [b] $P < 0.05$.

determinants for calcicludine block (*19*); and (3) calcicludine is a highly basic peptide toxin that possesses 12 positively charged lysine and arginine residues and only 2 acidic glutamate residues. Because basic residues of the BPTI/Kunitz dendrotoxins are known to interact with acidic residues in the S5/P segment of the outer vestibule of K^+ channels (*24*, *25*), we reasoned that similar interactions would be important for calcicludine binding to $Ca_V1.2$. In the following sections, we use site-directed mutagenesis, radioligand binding, and whole-cell patch-clamp electrophysiology to localize individual molecular determinants for calcicludine binding.

Acidic Residues Proximal to the Extracellular Portion of IIIS5 Are Important Binding Determinants for [^{3}H]PN200-110. The screen for amino acid residues critical for calcicludine binding was initiated by changing all nine acidic residues located in the IIIS5/P segment to alanine in three groups of three, resulting in the mutants Mut-A, Mut-B, and Mut-C (Figure 2A). Amino acids were changed to alanine in these studies because alanine substitutions eliminate the acidic properties of the substituted residues without causing global conformational changes in the channel protein (*26*). Initially, K_{DHP} values were determined by performing saturation binding experiments on membranes derived from cells expressing wild-type and all three mutant Ca^{2+} channels using the DHP antagonist [^{3}H]PN200-110. Figure 2B demonstrates that [^{3}H]PN200-110 binds to a single population of sites on membranes expressing wild-type $Ca_V1.2$ channels with a dissociation constant of 367 pM. In contrast, K_{DHP} for [^{3}H]PN200-110 binding to Mut-A membranes is increased to 1.7 nM (i.e., 4.5-fold larger than that of the wild type). K_{DHP} values for Mut-B and Mut-C are similar to that of the wild type (Figure 2C).

Three Acidic Amino Acid Residues, Glu-1122, Asp-1127, and Asp-1129, Positioned Proximal to the Pore Helix in Domain III Are Important for Calcicludine Binding to $Ca_V1.2$ Channels. The levels of [^{3}H]PN200-110 binding to membranes prepared from cells expressing Mut-A, Mut-B, and Mut-C channels were compared to that of the wild type in the presence of various concentrations of calcicludine using Scheme 1. In contrast to the wild type, DHP binding to Mut-A and Mut-C membranes is completely insensitive to calcicludine at concentrations up to 3 μM (Figure 3A). Calcicludine enhances [^{3}H]PN200-110 binding to Mut-B membranes with values for K_{CaC} and α similar to that determined for the wild type (Figure 3A; Table 1). Because block of Mut-A (but not Mut-C) currents by calcicludine is indistinguishable from that of wild type (Figure 5A), efforts to localize individual determinants critical for calcicludine binding and block were limited to the segment spanning Mut-C.

Three mutant channels containing single amino acid substitutions corresponding to those made in Mut-C, E1122A, D1127A, and D1129A, were analyzed to determine which are important for modulating DHP binding and channel block (Figure 3B, Table 1). As expected, K_{DHP} values for all three mutant channels are similar to those of the wild type and Mut-C (Table 1). The ability of calcicludine to increase [^{3}H]-PN200-110 binding to the mutant channels was assessed as described above. Because of the relatively large increases in K_{CaC} and the high cost of calcicludine, it was not possible to maximize the effect calcicludine has on DHP binding to

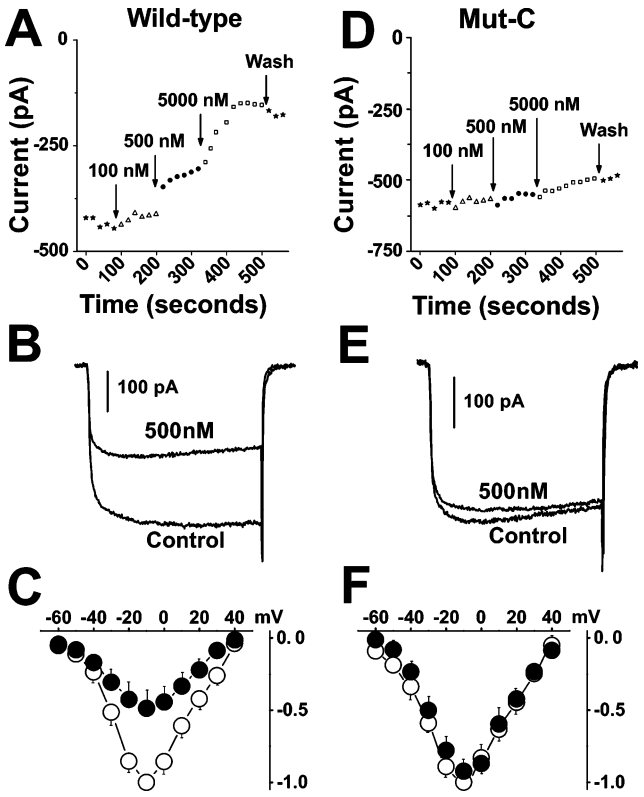

FIGURE 4: Mut-C channels are insensitive to block by calcicludine. (A and D) Peak amplitudes of Ba^{2+} currents evoked by 300 ms step depolarizations from −100 to −10 mV every 20 s from cells expressing wild-type (A) and Mut-C (D) Ca^{2+} channels in the presence of 0, 100, 500, and 5000 nM calcicludine. Note that Mut-C currents are insensitive to block by calcicludine. (B and E) Sample traces resulting from voltage steps from −100 to −10 mV in the absence and presence of 500 nM calcicludine. (C and F) Current−voltage relationships in the absence and presence of calcicludine were generated by depolarizing cells from a holding potential of −100 mV to 300 ms step depolarizations to potentials ranging from −60 to +80 mV. Peak currents were plotted against corresponding test voltages to give the current−voltage relationship ($I - V$). These data were fit using the equation, $I = G(V_m - V_{rev})/(1 + \exp[(V_h - V_m)/k])$, where G is the maximal slope conductance, V_{rev} is the reversal potential, V_m is the membrane potential, V_h is the half activation potential, and k is the slope factor. $I - V$ measurements were made in each cell in the absence and presence of calcicludine, and were normalized by dividing the peak current at each step potential by the peak of the fit through $I - V$ data acquired in the absence of calcicludine. Current voltage relationships indicate that the gross gating properties of Mut-C (F) are similar to that of the wild type (D).

E1122A, D1127A, and D1129A membranes. Therefore, curve fitting data from the mutant channels proved unreliable. To circumvent this limitation, the fits through the mutant data points (solid lines) were constructed using K_{CaC} values determined using the whole-cell patch-clamp experiments described below (Figure 5 and Table 1). Initially, the value for the cooperativity factor, α, was set to equal 0.48 (i.e., the same value as that of the wild type). The binding data for the wild type, E1122A, and D1129A were fit reasonably well using these constraints. This was not the case for D1127A (dashed line). It was necessary to increase α from 0.48 to 0.75 to obtain a reasonable fit through the data for D1127A (arrows). These results suggest that positively charged residues on calcicludine interact with Glu-1122, Asp-1127, and Asp-1129 in the outer vestibule of domain III of

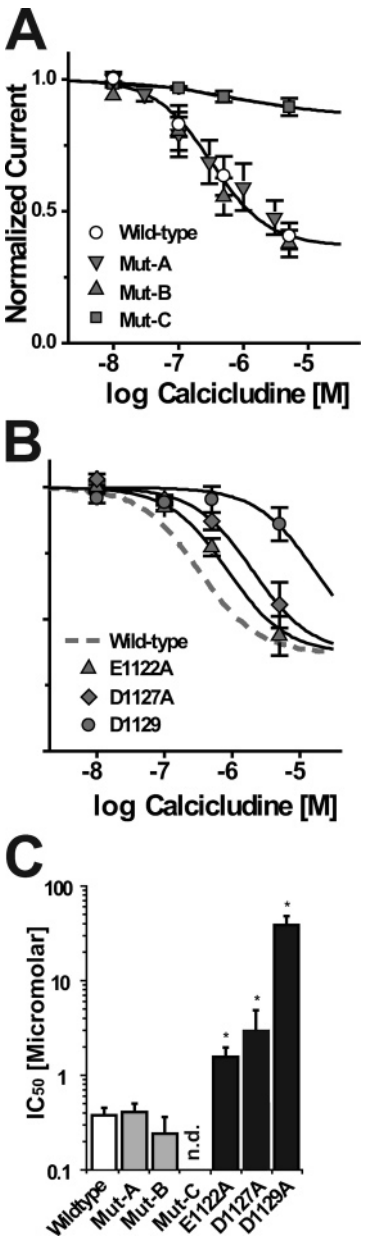

FIGURE 5: Glu-1122, Asp-1127, and Asp-1129 confer the channel's sensitivity to block by calcicludine. Currents through Mut-C, but not Mut-A or Mut-B, are insensitive to block by calcicludine. (A) The fraction of wild-type, Mut-A, Mut-B, and Mut-C current remaining after the application of the indicated concentrations of calcicludine ($I/I_{no\ drug}$) is plotted. The lines are logistic fits through the wild type (○) and Mut-C (■). Only 63% of the maximal Ba^{2+} current through wild-type channels is blocked by saturating concentrations of calcicludine. Data for Mut-A and Mut-B fit nicely with the same logistic function used to fit the wild-type data. Data are summarized in panel C and Table 1; wild-type ($n = 19$), Mut-A ($n = 4$), Mut-B ($n = 3$), and Mut-C ($n = 7$). (B) Ba^{2+} currents through E1122A, D1127A, and D1129A channels exhibit a reduced sensitivity to block by calcicludine. The fraction of Ba^{2+} current remaining ($I/I_{no\ drug}$) after the addition of 0, 100, 500, and 5000 nM calcicludine to wild-type and mutant Ca^{2+} channels is plotted. Best fits through the data were made assuming a Hill coefficient of 1.0 and, as was observed for wild-type (panel A), that a maximum of 63% of the total current is blocked at saturating concentrations of calcicludine; wild-type ($n = 19$), E1122A ($n = 6$), D1127A ($n = 6$), and D1129A ($n = 4$). (C) Summary of data depicted in panels A and B (also see Table 1). An IC_{50} value for Mut-C could not be determined (n.d.). IC_{50} values from these experiments were used to generate fits through the binding data shown in Figure 3B (see text and footnote to Table 1 for details). The statistical significance of the observed differences between the blocking parameters of wild-type and mutant channels was evaluated using a 2-tailed Students t-test. Patch-clamp data are the means ± SEM, and significance was set at $P < 0.05$ (*). Error bars smaller than symbols do not appear in the Figure.

$Ca_V1.2$ and that Asp-1127 may play an additional role in coupling DHP binding to calcicludine binding.

Glu-1122, Asp-1127, and Asp-1129 Confer the Channel's Sensitivity to Block by Calcicludine. In Figure 4, whole-cell patch-clamp electrophysiology was used to characterize the basic functional and pharmacological properties of cells expressing wild-type and mutant channels. Initially, it was found that of Mut-A, Mut-B, and Mut-C, only Mut-C is insensitive to block by calcicludine (Figure 4). In Figure 4A and D, cells were depolarized every 20 s to −10 mV from a holding potential of −100 mV in the presence of 0, 100, 500, and 5000 nM calcicludine. Cells expressing wild-type channels are blocked by calcicludine with an IC_{50} of 322 nM, and in contrast to the findings of Stotz et al. (*19*) and Schweitz et al. (*16*), a small statistically insignificant amount of current (∼8%) is typically recovered upon washout of the toxin. Consistent with the findings of Stotz et al. (*19*), but not Schweitz et al. (*16*), only 63% of the wild-type current is sensitive to calcicludine. Also in agreement with Stotz, et al. (*19*), we did not observe a change in the half-activation potential of wild-type or mutant $Ca_V1.2$ currents upon application of 500 nM calcicludine (Figure 4C). In contrast to the wild type, Mut-A, and Mut-B, Mut-C is resistant to block by calcicludine at concentrations up to 5000 nM (Figure 4D, E, and F). Thus, the IC_{50} for the block of Mut-C by calcicludine must be at least 500 μM. These findings are summarized in Figure 5A. Block of currents through the single mutants, E1122A, D1127A, and D1129A, by calcicludine were increased 3.5-, 5.0-, and ∼65-fold, respectively, above that of the wild type, indicating that all three residues contribute to calcicludine binding (Figure 5B and C).

DISCUSSION

Here, we used calcicludine, a toxin from the venom of the green mamba snake, as a molecular probe to obtain a deeper understanding of the mechanism by which DHP antagonists block L-type Ca^{2+} channels. We found that DHP, [^{3}H]PN200-110, binds cooperatively with calcicludine to cardiac $Ca_V1.2$ Ca^{2+} channels expressed in HEK 293 cells (Figure 1). The positive cooperativity observed between calcicludine and [^{3}H]PN200-110 can only occur if both ligands bind simultaneously to the channel; therefore, calcicludine appears to be an *allosteric* modulator of DHP binding. Scheme 1 was developed to model the interactions between DHP and calcicludine binding. Neutralization of three acidic amino acid residues, Glu-1122, Asp-1127, and Asp-1129, located adjacent to the pore helix of repeat III results in mutant channels that have reduced sensitivity to block by calcicludine (Figures 4 and 5; Table 1). Similar results were obtained using an allosteric binding assay (Figure 3), where data were fit nicely using IC_{50} values for half-maximal block of Ba^{2+} currents through the mutant channels. These independent experimental approaches (one a DHP-independent functional assay and the other a DHP-dependent binding assay) suggest that calcicludine directly interacts with acidic amino acid residues, Glu-1122, Asp-1127, and Asp-1129. Below, we use a *domain-interface model* to explain the molecular details that underlie the positive cooperativity between the DHP and calcicludine binding sites and propose a molecular mechanism to explain how calcicludine and DHPs modulate Ca^{2+} channel activity.

Molecular Basis for Positive Cooperativity between DHP and Calcicludine Binding. The domain-interface theory predicts that allosteric ligands bind at structural interfaces, possibly because the receptor protein is most flexible in such regions (*7*, *27*−*31*). The domain-interface theory can be used to explain how the calcicludine and DHP binding sites are allosterically coupled as well. Our findings indicate that calcicludine binds to a peptide segment including and proximal to the pore helix in repeat III. Structural models of L-type Ca^{2+} channels predict that this segment is nestled between IIIS5, IIIS6, and IVS6 (*32*−*34*). Thus, although DHPs and calcicludine possess very distinct chemical and physical properties, their respective binding sites share an important feature: both binding sites are located at the interface between repeats III and IV. Binding of either ligand would be expected to alter the interactions between repeats III and IV and, consequently, the functional properties of the channel. The positive cooperativity between DHP antagonists and calcicludine likely occurs because the two ligands bind at the interface between the pore motifs of repeats III and IV and stabilize a common conformational state in the outer pore. Consequently, DHP binding becomes more energetically favorable in the presence of calcicludine and, though not tested, vice versa. This model for DHP and calcicludine binding predicts that interdomain movements resulting from the binding of either ligand shift the channel from a permeant state to a blocked state. This scenario is consistent with our previous reports that DHP antagonists block Ca^{2+} channels by promoting structural rearrangements in the outer pore (*12*). In these studies, we postulated that the outer pore of an activated channel switches between conducting and nonconducting blocked states and that the overall open probability (P_O) of the channel is determined by the probability that the inner gate is open and whether the outer pore is in its conducting or nonconducting state. These findings further suggest that DHP antagonists (and perhaps calcicludine) block Ca^{2+} currents by promoting structural rearrangements in the outer pore that correspond to the nonconducting state.

The domain-interface model for the allosteric interactions between the calcicludine and DHP receptor sites is further supported by the observation that the amino acid substitutions in Mut-A located in the extracellular loop proximal to IIIS5 are important determinants for DHP binding (Figure 2D; Table 1). The DHP receptor site is thought to lie deep within the lipid bilayer, yet the segment containing the amino acid substitutions in Mut-A is predicted to be extracellular. Thus, the DHP receptor site and the amino acid residues altered in Mut-A are not spatially oriented in a way that would allow the two regions of the channel to form a single binding site. Interestingly, the dissociation constant for [^{3}H]PN200-110 binding (i.e., K_{DHP}) to Mut-A membranes is 4.5-fold larger than that of the wild type (Figure 2). Because the sensitivity of Mut-A currents to calcicludine is similar to that of the wild type (Figure 3A), it appears that the dissociation constant for calcicludine binding to Mut-A, K_{CaC}, is unaltered but that K_{DHP} increases 4.5-fold, and the cooperativity between the DHP and calcicludine binding sites, α, increases from 0.5 to ∼1.

It seems unlikely that the amino acid residues substituted in Mut-A contribute directly to the formation of the DHP receptor site; therefore, these substitutions may affect K_{DHP}

and α via an allosteric mechanism. The most reasonable explanation for these findings is that one or more of the three acidic amino acid residues substituted in Mut-A is important for stabilizing the interaction between repeats III and IV in a way that is favorable for DHP binding. Amino acid substitutions at this position would then destabilize these interactions, and DHP binding would become less favorable. Thus, drugs that target amino acid residues that lie within the Mut-A peptide segment may function as allosteric modulators of voltage-gated Ca^{2+} channels.

Calcicludine and δ-Dendrotoxin Share Similar Pharmacological Properties. The selectivity filters of $Ca_V1.2$ differ from that of KcsA and other K^+ channels, but the gross structural features of their respective pores are predicted to be conserved. Therefore, we compared the results of our localization studies with those of Imredy et al. who characterized the binding of *δ*-dendrotoxin to the inward rectifying ($K_{ir}1.1$) and voltage-gated ($K_V1.1$) K^+ channels (*24*, *25*). Like calcicludine, *δ*-dendrotoxin is a member of the BPTI/Kunitz-like toxin family (*15*, *18*). Neutralization of Glu-123 of $K_{ir}1.1$ results in a mutant channel with an IC_{50} for half-maximal block by *δ*-dendrotoxin that is more than 250-fold larger than that of the wild type (*24*), and substitution of alanine for Asp-431 results in a 160-fold increase in the IC_{50} for the half-maximal block of $K_V1.1$ channels by *δ*-dendrotoxin (*25*). As with Glu-1122, Asp-1127, and Asp-1129 of $Ca_V1.2$, Glu-123 of $K_{ir}1.1$ and Asp-431 of $K_V1.1$ are located within and are proximal to the pore helix. Therefore, the interactions between calcicludine and *δ*-dendrotoxin and their respective channel targets appear to be conserved.

In their later study, Imredy and Mackinnon (*25*) found that one face of *δ*-dendrotoxin interacts off-center in the pore with three residues on the turret and an aspartate residue (Asp-431 of $K_V1.1$) positioned in the outer portion of the pore helix between two K^+ channel subunits. The similarities between our results and those of Imredy and MacKinnon (*25*) and Stotz et al. (*19*) indicate that calcicludine and *δ*-dendrotoxin bind to their respective receptor sites in a similar manner and suggest that the two toxins may alter channel activity via a similar *modus operandi*, that is, by partially occluding the permeation pathway (*19*, *24*, *25*). As noted by Stotz et al. (*19*), our findings can also be explained by an allosteric model. The selectivity filter appears to be a dynamic structure that undergoes structural rearrangements in response to changes in channel activity. For example, a pore containing no divalent cations is predicted to be 6 Å in diameter (*35*) and freely conducts monovalent cations. Occupancy of the pore by a single divalent cation introduces electrostatic forces that cause the selectivity filter to collapse to 2.8 Å (*33*), a structure that corresponds to the nonconducting blocked state stabilized by DHP antagonists (*12*). Occupancy by a second divalent cation introduces repulsive forces in the selectivity filter and stabilizes a state that conducts divalent cations. Calcicludine binding to the outer vestibule of the pore may promote a pore structure that is structurally analogous to the nonconducting blocked state stabilized by DHP antagonists.

ACKNOWLEDGMENT

We thank Cara Martinez-Williams for technical assistance.

REFERENCES

1. Hille, B. (2001) *Ion Channels of Excitable Membranes*, 3rd ed., Sinaur Associates, Inc., Sunderland, MA.
2. Herbert, L. G. (1994) Membrane pathways for drug/ion channel interactions: molecular basis for pharmacokinetic properties, *Drug Dev. Res. 33*, 214−224.
3. Bangalore, R., Baindur, N., Rutledge, A., Triggle, D. J., and Kass, R. S. (1994) L-type calcium channels: asymmetrical intramembrane binding domain revealed by variable length, permanently charged 1,4-dihydropyridines, *Mol. Pharmacol. 46*, 660−666.
4. He, M., Bodi, I., Mikala, G., and Schwartz, A. (1997) Motif III S5 of L-type calcium channels is involved in the dihydropyridine binding site. A combined radioligand binding and electrophysiological study, *J. Biol. Chem. 272*, 2629−2633.
5. Mitterdorfer, J., Wang, Z., Sinnegger, M. J., Hering, S., Striessnig, J., Grabner, M., and Glossmann, H. (1996) Two amino acid residues in the IIIS5 segment of L-type calcium channels differentially contribute to 1,4-dihydropyridine sensitivity, *J. Biol. Chem. 271*, 30330−30335.
6. Peterson, B. Z., Johnson, B. D., Hockerman, G. H., Acheson, M., Scheuer, T., and Catterall, W. A. (1997) Analysis of the dihydropyridine receptor site of L-type calcium channels by alanine-scanning mutagenesis, *J. Biol. Chem. 272*, 18752−18758.
7. Peterson, B. Z., Tanada, T. N., and Catterall, W. A. (1996) Molecular determinants of high affinity dihydropyridine binding in L-type calcium channels, *J. Biol. Chem. 271*, 5293−5296.
8. Schuster, A., Lacinova, L., Klugbauer, N., Ito, H., Birnbaumer, L., and Hofmann, F. (1996) The IVS6 segment of the L-type calcium channel is critical for the action of dihydropyridines and phenylalkylamines, *EMBO J. 15*, 2365−2370.
9. Mitterdorfer, J., Sinnegger, M. J., Grabner, M., Striessnig, J., and Glossmann, H. (1995) Coordination of Ca2+ by the pore region glutamates is essential for high-affinity dihydropyridine binding to the cardiac Ca2+ channel alpha 1 subunit, *Biochemistry 34*, 9350−9355.
10. Peterson, B. Z., and Catterall, W. A. (1995) Calcium binding in the pore of L-type calcium channels modulates high affinity dihydropyridine binding, *J. Biol. Chem. 270*, 18201−18204.
11. Wang, X., Ponoran, T. A., Rasmusson, R. L., Ragsdale, D. S., and Peterson, B. Z. (2005) Amino acid substitutions in the pore of the CaV1.2 calcium channel reduce barium currents without affecting calcium currents, *Biophys. J. 89*, 1731−1743.
12. Peterson, B. Z., and Catterall, W. A. (2006) Allosteric interactions required for high-affinity binding of dihydropyridine antagonists to Ca(V)1.1 channels are modulated by calcium in the pore, *Mol. Pharmacol. 70*, 667−675.
13. Menez, A. (2002) *Perspectives in Molecular Toxicology*, John Wiley & Sons, Ltd., West Sussex, U.K.
14. Swaminathan, P., Hariharan, M., Murali, R., and Singh, C. U. (1996) Molecular structure, conformational analysis, and structure-activity studies of dendrotoxin and its homologues using molecular mechanics and molecular dynamics techniques, *J. Med. Chem. 39*, 2141−2155.
15. Gilquin, B., Lecoq, A., Desne, F., Guenneugues, M., Zinn-Justin, S., and Menez, A. (1999) Conformational and functional variability supported by the BPTI fold: solution structure of the Ca2+ channel blocker calcicludine, *Proteins 34*, 520−532.
16. Schweitz, H., Heurteaux, C., Bois, P., Moinier, D., Romey, G., and Lazdunski, M. (1994) Calcicludine, a venom peptide of the Kunitz-type protease inhibitor family, is a potent blocker of high-threshold Ca2+ channels with a high affinity for L-type channels in cerebellar granule neurons, *Proc. Natl. Acad. Sci. U.S.A. 91*, 878−882.
17. Zupunski, V., Kordis, D., and Gubensek, F. (2003) Adaptive evolution in the snake venom Kunitz/BPTI protein family, *FEBS Lett. 547*, 131−136.
18. Harvey, A. L. (2001) Twenty years of dendrotoxins, *Toxicon 39*, 15−26.
19. Stotz, S. C., Spaetgens, R. L., and Zamponi, G. W. (2000) Block of voltage-dependent calcium channel by the green mamba toxin calcicludine, *J. Membr. Biol. 174*, 157−165.
20. Wei, X. Y., Perez-Reyes, E., Lacerda, A. E., Schuster, G., Brown, A. M., and Birnbaumer, L. (1991) Heterologous regulation of the cardiac Ca2+ channel alpha 1 subunit by skeletal muscle beta and gamma subunits. Implications for the structure of cardiac L-type Ca2+ channels, *J. Biol. Chem. 266*, 21943−21947.

21. Perez-Reyes, E., Castellano, A., Kim, H. S., Bertrand, P., Baggstrom, E., Lacerda, A. E., Wei, X. Y., and Birnbaumer, L. (1992) Cloning and expression of a cardiac/brain beta subunit of the L-type calcium channel, *J. Biol. Chem. 267*, 1792−1797.
22. Tomlinson, W. J., Stea, A., Bourinet, E., Charnet, P., Nargeot, J., and Snutch, T. P. (1993) Functional properties of a neuronal class C L-type calcium channel, *Neuropharmacology 32*, 1117−1126.
23. Wang, X., Ponoran, T. A., Rasmusson, R. L., Ragsdale, D. S., and Peterson, B. Z. (2005) Amino acid substitutions in the pore of the Ca(V)1.2 calcium channel reduce barium currents without affecting calcium currents, *Biophys. J. 89*, 1731−1743.
24. Imredy, J. P., Chen, C., and MacKinnon, R. (1998) A snake toxin inhibitor of inward rectifier potassium channel ROMK1, *Biochemistry 37*, 14867−14874.
25. Imredy, J. P., and MacKinnon, R. (2000) Energetic and structural interactions between delta-dendrotoxin and a voltage-gated potassium channel, *J. Mol. Biol. 296*, 1283−1294.
26. Blaber, M., Zhang, X. J., and Matthews, B. W. (1993) Structural basis of amino acid alpha helix propensity, *Science 260*, 1637−1640.
27. Barford, D., and Johnson, L. N. (1989) The allosteric transition of glycogen phosphorylase, *Nature 340*, 609−616.
28. Kantrowitz, E. R., and Lipscomb, W. N. (1990) *Escherichia coli* aspartate transcarbamoylase: the molecular basis for a concerted allosteric transition, *Trends Biochem. Sci. 15*, 53−59.
29. Karlin, A., and Akabas, M. H. (1995) Toward a structural basis for the function of nicotinic acetylcholine receptors and their cousins, *Neuron 15*, 1231−1244.
30. Zhang, Y., Liang, J. Y., Huang, S., and Lipscomb, W. N. (1994) Toward a mechanism for the allosteric transition of pig kidney fructose-1,6-bisphosphatase, *J. Mol. Biol. 244*, 609−624.
31. Lipkind, G. M., and Fozzard, H. A. (2003) Molecular modeling of interactions of dihydropyridines and phenylalkylamines with the inner pore of the L-type Ca2+ channel, *Mol. Pharmacol. 63*, 499−511.
32. Doyle, D. A., Morais Cabral, J., Pfuetzner, R. A., Kuo, A., Gulbis, J. M., Cohen, S. L., Chait, B. T., and MacKinnon, R. (1998) The structure of the potassium channel: molecular basis of K+ conduction and selectivity, *Science 280*, 69−77.
33. Lipkind, G. M., and Fozzard, H. A. (2001) Modeling of the outer vestibule and selectivity filter of the L-type Ca2+ channel, *Biochemistry 40*, 6786−6794.
34. Zhorov, B. S., Folkman, E. V., and Ananthanarayanan, V. S. (2001) Homology model of dihydropyridine receptor: implications for L-type Ca(2+) channel modulation by agonists and antagonists, *Arch. Biochem. Biophys. 393*, 22−41.
35. McCleskey, E. W., and Almers, W. (1985) The Ca channel in skeletal muscle is a large pore, *Proc. Natl. Acad. Sci. U.S.A. 82*, 7149−7153.

BI7001696